

See discussions, stats, and author profiles for this publication at: <https://www.researchgate.net/publication/231634801>

# The Structure of Alanine Based Tripeptides in Water and Dimethyl Sulfoxide Probed by Vibrational Spectroscopy

ARTICLE *in* THE JOURNAL OF PHYSICAL CHEMISTRY B · DECEMBER 2002

Impact Factor: 3.3 · DOI: 10.1021/jp026958t

CITATIONS

77

READS

36

5 AUTHORS, INCLUDING:



**Laurence A Nafie**

Syracuse University

306 PUBLICATIONS 7,512 CITATIONS

SEE PROFILE



**Qing Huang**

Chinese Academy of Sciences

100 PUBLICATIONS 1,484 CITATIONS

SEE PROFILE



**Reinhard Schweitzer-Stenner**

Drexel University

219 PUBLICATIONS 4,369 CITATIONS

SEE PROFILE

# The Structure of Alanine Based Tripeptides in Water and Dimethyl Sulfoxide Probed by Vibrational Spectroscopy

Fatma Eker,<sup>‡</sup> Xiaolin Cao,<sup>§</sup> Laurence Nafie,<sup>§</sup> Qing Huang,<sup>†</sup> and Reinhard Schweitzer-Stenner<sup>\*,†</sup>

Departments of Chemistry and Biology, University of Puerto Rico, Río Piedras Campus, San Juan, PR00931, and Department of Chemistry, Syracuse University, Syracuse, New York 13244

Received: September 10, 2002; In Final Form: November 1, 2002

We have measured the band profile of amide I in the infrared, isotropic, and anisotropic Raman spectra of cationic L-alanyl-D-alanyl-L-alanine, L-lysyl-L-alanine-L-alanine, and L-seryl-L-alanine-L-alanine in D<sub>2</sub>O. Additionally, we recorded spectra of N-acetyl-L-alanyl-L-alanine in D<sub>2</sub>O and in DMSO-*d*<sub>6</sub>. The respective intensity ratios of the two amide I bands depend on excitonic coupling between the amide I modes of the two peptides. These intensity ratios were obtained from a spectral decomposition and then used to determine the dihedral angles between the peptide groups by means of a recently developed algorithm (Schweitzer-Stenner, *Biophys. J.*, 83, 83, 523, 2002). The validity of the obtained structures was checked by measuring the vibrational circular dichroism of the amide I bands. L-Lysyl-L-alanyl-L-alanine, L-seryl-L-alanyl-L-alanine, and acetyl-L-alanyl-L-alanine adopt structures similar to that observed for L-alanyl-L-alanyl-L-alanine. This suggests that the N-terminal residues do not significantly influence the dihedral angles between the two peptide groups. If one assumes a single dominant conformer, one obtains a  $\beta$ -helix or extended polyproline II conformation, while a two-conformer model yields coexisting polyproline II and extended  $\beta$ -type conformers. Acetyl-L-alanyl-L-alanine in DMSO-*d*<sub>6</sub> adopts a  $\beta$ -sheet-like structure. Its amide I bands are significantly less broadened than those observed with D<sub>2</sub>O solvent. Our results show that hydrogen bonding between the peptide and water molecules contributes significantly to the inhomogeneous broadening of amide I bands and stabilizes the polyproline II conformation.

## Introduction

Vibrational spectroscopies such as infrared (FTIR) and Raman spectroscopy are frequently used to quantify the contribution of distinct secondary structure motifs to the overall protein structure.<sup>1–3</sup> In addition, one can probe those amino acid residues, the spectral lines of which are clearly discernible in even complex spectra, e.g., the IR band of the antisymmetric carboxylate stretching vibrations<sup>4</sup> or Raman lines of W, Y, and F that are resonance enhanced with UV excitation.<sup>5</sup> Some more detailed information can be inferred from vibrational circular dichroism (VCD)<sup>6</sup> and Raman optical activity (ROA) spectra.<sup>7,8</sup> Generally, however, vibrational spectroscopy is still not in a position to compete with NMR and X-ray crystallography with respect to structure resolution. This is unfortunate, because both Raman and IR offer a much larger time window for investigating dynamic processes ( $>10^{-12}$  s), which makes these techniques suitable to study structural conversions and protein folding.<sup>9,10</sup> Recently, progress has been made in utilizing vibrational spectroscopy to determine the structure of tripeptides in water. First, Woutersen and Hamm<sup>11</sup> employed 2D coherent femtosecond IR spectroscopy to obtain the energy  $\Delta$  of excitonic coupling between the amide I modes of the two peptide groups in trialanine (Figure 1) and the orientational angle  $\bar{\theta}$  between their transition dipole moments. The dihedral angles between

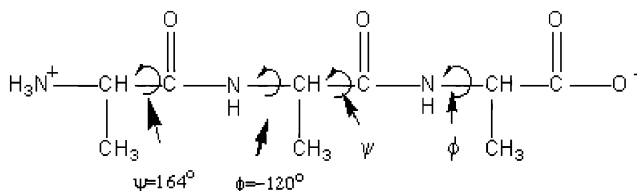


**Figure 1.** Chemical structure of zwitterionic AAA and representation of the dihedral angles obtained from the analysis of the amide I band profiles in IR absorption and Raman scattering (Eker et al.<sup>21</sup>).

the two peptide groups were then obtained as follows. First, the authors calculated  $\bar{\theta}$  as a function of the dihedral angles  $\phi$  and  $\psi$  between the peptide groups. The corresponding contour plots are shown in Figure 2. Second, they utilized the  $\phi$  and  $\psi$  dependence of  $\Delta$  which Torri and Tasumi<sup>12</sup> had obtained from ab initio calculations on a blocked triglycine analogue. Third, they compared the results of these calculations with their experimentally obtained parameter values. Eventually, this yielded the dihedral angles of cationic trialanine in D<sub>2</sub>O, i.e.,  $(\phi, \psi) = (-60^\circ, 140^\circ)$ . These angles reflect a polyproline II (PII) of 3<sub>1</sub> helix structure which Tiffani and Krimm<sup>13</sup> have hypothesized to be the dominant motif in so-called coiled structures of polypeptides and proteins.

Another approach based on vibrational spectroscopies was reported by Schweitzer-Stenner et al.<sup>14</sup> These authors explored the excitonic states of amide I in all protonation states of AAA in D<sub>2</sub>O by measuring the respective FTIR and polarized Raman spectra. From the latter they obtained the isotropic and anisotropic scattering in the amide I region. The former was used to determine the coupling energy  $\Delta$  and the degree of mixing between the two interacting excited amide I states. In the second

\* Corresponding author. Department of Chemistry, University of Puerto Rico, Río Piedras Campus, P.O. Box 23346, San Juan, PR 00931, USA. Phone: 787-764-0000 ext. 2417. Fax: 787-756-8242. E-mail: rstenner\_upr\_chemistry@gmx.net

<sup>†</sup> Department of Chemistry, University of Puerto Rico.

<sup>‡</sup> Department of Biology, University of Puerto Rico.

<sup>§</sup> Department of Chemistry, Syracuse University.

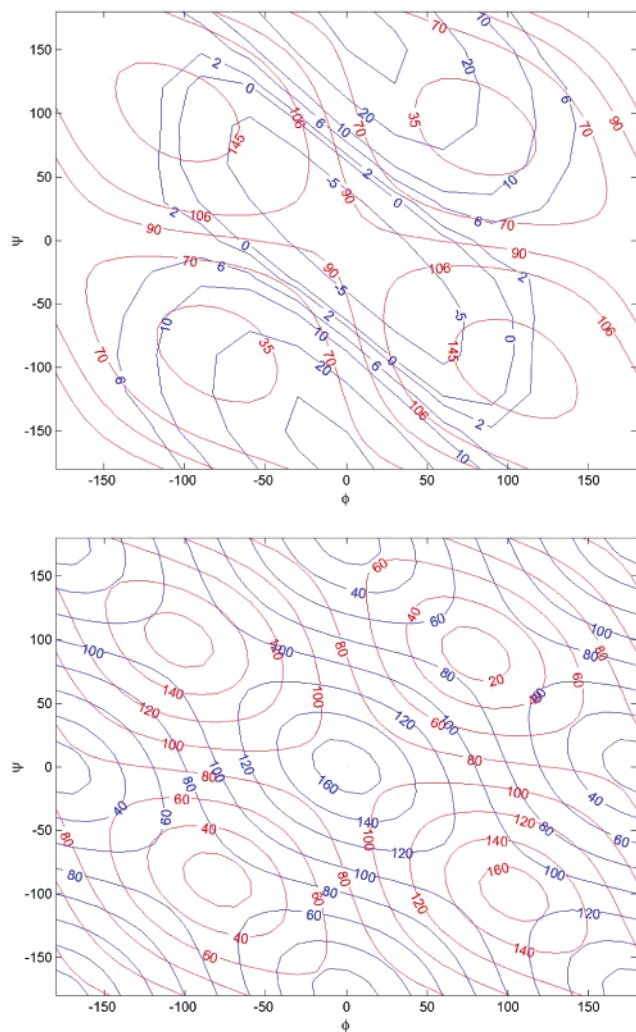


**Figure 2.** (a) Contour plots of the coupling constant  $\Delta$  (blue, in  $\text{cm}^{-1}$ ) and the orientational angle  $\bar{\theta}(\phi, \psi)$  (red, in deg) as functions of the dihedral angles  $\phi$  and  $\psi$ . The  $\bar{\theta}(\phi, \psi)$  dependence was calculated using the formalism outlined in ref 16. The data for the  $\Delta(\phi, \psi)$  contours were calculated based on the force constant reported in ref 12 (the data were kindly provided by Dr. Torii). (b) Contour plots of the orientational angles  $\theta$  (blue) and  $\bar{\theta}$  (red) (both in deg) as functions of the dihedral angles  $\phi$  and  $\psi$  calculated by means of the formalisms reported in ref 16.

step, they used the FTIR spectrum of amide I to determine the orientational angle  $\bar{\theta}$  between the transition dipole moments. Like Woutersen and Hamm<sup>11,15</sup> they utilized the contour plots in Figure 2 to derive the dihedral angles. For the cationic state of AAA they thus obtained  $(\phi, \psi) = (-66^\circ, 140^\circ)$ , which is very close to the values of Woutersen and Hamm. Moreover, they found that the deprotonation of the terminal groups does not cause any significant structural changes.

Recently, Schweitzer-Stenner<sup>16</sup> extended the above approach by additionally using the anisotropic Raman scattering of amide I to determine the orientational angle  $\theta$  between the peptide groups. The obtained values for  $\bar{\theta}$  and  $\theta$  were then used to determine  $\phi$  and  $\psi$  directly from the spectroscopic data rather than from the results of ab initio calculations. This yielded a somewhat more extended structure for AAA (i.e.,  $(\phi, \psi) = (-126^\circ, 178^\circ)$  for the cationic state), which can be described as a  $\beta$ -helix<sup>1</sup> or as a very extended PII conformation.

In the present study we use the algorithm of Schweitzer-Stenner<sup>16</sup> to compare the structure of L-alanyl-L-alanyl-L-alanine (AAA), L-lysyl-L-alanyl-L-alanine (KAA), and L-seryl-L-alanyl-L-alanine (SAA) in  $\text{D}_2\text{O}$  to determine the influence of the

N-terminal amino acid residue on the dihedral angles between the peptide groups. Moreover, we investigated the structure of N-acetyl-L-alanyl-L-alanine in  $\text{H}_2\text{O}$  and in  $\text{DMSO}-d_6$  to determine the influence of the solvent on the spectral properties and the structure of alanine-based tripeptides.

## Material and Methods

**Materials.** N-Acetyl-L-alanyl-L-alanine (AcAA) was purchased from Bachem Bioscience Inc. (>98% purity) and used without further purification. L-Lysyl-L-alanyl-L-alanine (KAA) and L-seryl-L-alanyl-L-alanine (SAA) were synthesized by Peptides International (Louisville, KY).  $\text{NaClO}_4$  was obtained from Sigma-Aldrich Chemical Company (St. Louis, MO). Dimethyl sulfoxide- $d_6$  was purchased from Cambridge Isotope Laboratories, Inc. (Andover, MA). All chemicals were of analytical grade. The peptides were dissolved in  $\text{D}_2\text{O}$ ,  $\text{H}_2\text{O}$ , and  $\text{DMSO}-d_6$  at a concentration between 0.05 and 0.5 M. The pD and pH of the solutions were adjusted by adding small aliquots of DCl or NaOD and HCl or NaOH respectively to obtain the cationic, zwitterionic, and anionic state of the peptides. The pD values were determined by utilizing the method of Glasoe and Long<sup>17</sup> to correct the values obtained from pH electrode measurements. For the Raman experiments the solvent contained 0.25–0.1 M  $\text{NaClO}_4$ , whose  $934\text{ cm}^{-1}$  Raman band was used as an internal standard.<sup>18</sup>

**Theoretical Methods. Excitonic Coupling of Amide I Modes.** The theory used to obtain the dihedral angles of tripeptides from the amide I bands in their visible Raman and IR spectra have been described in detail elsewhere.<sup>16</sup> Only the basic principles are briefly summarized in the following.

We assume a two-oscillator model to describe the mixing between the two amide I modes of tripeptides by transition-dipole and through-bond coupling. The corresponding excitonic states are written as

$$\begin{aligned} |\chi_{-}\rangle &= \cos \nu |\chi_1\rangle - \sin \nu |\chi_2\rangle \\ |\chi_{+}\rangle &= \sin \nu |\chi_1\rangle + \cos \nu |\chi_2\rangle \end{aligned} \quad (1)$$

The parameter  $\nu$  describes the degree of mixing between the unperturbed states  $|\chi_1\rangle$  and  $|\chi_2\rangle$ , which is maximal for  $\nu = 45^\circ$ . This requires the unperturbed modes to be accidentally degenerated.  $|\chi_{+}\rangle$  and  $|\chi_{-}\rangle$  are the excitonic states of the in-phase (ip) and out-of-phase (oop) combination of the interacting modes. The relationship between  $\nu$  and the coupling energy  $\Delta$  is written as

$$\Delta = \frac{1}{2} \Delta_{\text{exp}} \sin 2\nu \quad (2)$$

where  $\Delta_{\text{exp}}$  denotes the experimental wavenumber difference between the two amide I bands.<sup>19</sup> The mixing parameter  $\nu$  can be determined from the intensity ratio  $R_{\text{iso}} = I_{\text{iso}}^{-}/I_{\text{iso}}^{+}$  of the two amide I bands in the spectrum of isotropic Raman scattering ( $I_{\text{iso}}^{-}$  and  $I_{\text{iso}}^{+}$  are the isotropic intensities of  $|\chi_{-}\rangle$  and  $|\chi_{+}\rangle$ ). In the next step we use the mixing parameter and the intensity ratio  $R_{\text{IR}} = I_{\text{IR}}^{-}/I_{\text{IR}}^{+}$  in the FTIR spectrum to obtain the angle  $\bar{\theta}$  between the transition dipole moments of amide I. Third, we made use of the fact that intensity ratio  $R_{\text{aniso}}$  of the amide I in anisotropic Raman spectrum depends on the mixing parameter and on the orientation angle  $\theta$  between the peptide normals. We calculated  $R_{\text{aniso}}$  as a function of  $\theta$  and compared the result with the respective experimental value. Thus, one generally obtains two values  $\theta_1$  and  $\theta_2$ , for which the experimental  $R_{\text{aniso}}$  value could be reproduced. In the final step, we calculate  $\theta$  and

**TABLE 1: Spectral and Structural Parameters of Cationic AAA,<sup>a</sup> AA<sup>DA</sup>,<sup>b</sup> KAA, and SAA Obtained from the Single-Conformer Analysis**

	AAA	AA <sup>DA</sup>	KAA	SAA
$\tilde{\nu}_-$ [cm <sup>-1</sup> ]	1652	1649	1650	1649
$\tilde{\nu}_+$ [cm <sup>-1</sup> ]	1676	1673	1672	1675
$\Gamma_{G-}$ [cm <sup>-1</sup> ] <sup>c</sup>	21.3	21.3	21.3	29.6
$\Gamma_{G+}$ [cm <sup>-1</sup> ] <sup>c</sup>	18.9	18.9	18.9	21.9
$R_{\text{iso}}$	0.39	0.45	0.45	0.52
$R_{\text{aniso}}$	1.16	1.2	1.36	1.13
$R_{\text{IR}}$	1.52	1.42	1.54	1.65
$\rho_-$	0.24	0.24	0.26	0.18
$\rho_+$	0.12	0.12	0.11	0.11
$\Delta$ [cm <sup>-1</sup> ] <sup>d</sup>	5.2	4.6	4.2	3.9
$\bar{\theta}$	119°	118°	124°	124°
$\theta$	124°	118°	114°	141°
$\phi$	-123°	115°	-118°	-122°
$\psi$	173°	-175°	160°	150°

<sup>a</sup> Taken from Schweitzer-Stenner.<sup>16</sup> <sup>b</sup> Taken from Eker et al.<sup>21</sup><sup>c</sup> Gaussian halfwidths. <sup>d</sup> Corrected values calculated by using eq 2.**TABLE 2: Structural Parameters of Cationic AAA,<sup>a</sup> AA<sup>DA</sup>,<sup>b</sup> KAA, and SAA Obtained from the Two-Conformer Analysis**

	AAA	AA <sup>DA</sup>	KAA	SAA
$R^c$	1	0.9	1	0.3
$\phi_1$	-60°	50°	-60°	-55.0°
$\psi_1$	150°	-140°	150°	145°
$\phi_2$	-160°	150°	-160°	-160°
$\psi_2$	150°	-155°	150°	145°

<sup>a</sup> Taken from Schweitzer-Stenner.<sup>16</sup> <sup>b</sup> Taken from Eker et al.<sup>21</sup> <sup>c</sup>  $R$  is the concentration ratio of conformer 1 (PII) to conformer 2 ( $\beta$ -like).

$\bar{\theta}$  as functions of the dihedral angles  $\phi$  and  $\psi$ . The corresponding contour plots are depicted in Figure 2b. By comparison with the  $\theta$  and  $\bar{\theta}$  values obtained from the experimental data, one generally obtains up to eight pairs of  $\phi, \psi$  values, four pairs corresponding to  $\bar{\theta}$  and  $\theta_1$  and the remaining four to  $\bar{\theta}$  and  $\theta_2$ . Up to six of these solutions can generally be excluded because they correspond to forbidden regions of the Ramachandran space. Moreover, as shown below, vibrational circular dichroism can be used in many cases to identify the correct  $\phi, \psi$  pair from the remaining solutions. All the mathematical details of our model are reported in ref 16.

A detailed estimation of the error intervals for the  $\phi$  and  $\psi$  values obtained from the IR and Raman data has been given in ref 27. We followed the same procedure to obtain the statistical errors for the dihedral angles of the tripeptides investigated in the present study (Tables 1 and 2). Due to the highly nonlinear propagation of errors, asymmetric error intervals are obtained.

**VCD Signal of Amide I.** In the absence of any intrinsic chirality (no VCD signal of the unperturbed amide I), excitonic coupling creates a VCD couplet. For a coupled oscillator one obtains for the rotational strength of  $|\chi_+\rangle$  and  $|\chi_-\rangle$ :<sup>20</sup>

$$R^\pm = \mp \frac{1}{2} \sin 2\nu \cdot \pi \tilde{\nu}_0 \vec{T}_{12} \cdot (\Delta\vec{\mu}_1 \times \Delta\vec{\mu}_2) \quad (3)$$

where  $\tilde{\nu}_0$  is the average wavenumber of the two amide I bands,  $\vec{T}_{12}$  is the distance vector between the two oscillators, and  $\Delta\vec{\mu}_{1,2}$  are their transition dipole moments. Chirality is brought about by the different orientation of the two transition dipoles, it disappears for  $\bar{\theta} = 0^\circ$ . Generally, eq 3 yields a negative signal for  $|\chi_-\rangle$  and a positive one of equal intensity for  $|\chi_+\rangle$  in the case of extended structures in the upper left square of the Ramachandran plot, while it is just the other way round if the structure is helical.<sup>6</sup>

As shown below, the amide I of the C-terminal group has some rotational strength depending on the protonation state. To

take this into account we modified eq 3 to obtain

$$R^- = \Delta\vec{\mu}_1 \Delta\vec{m}_1 \cos^2(\nu) - \frac{1}{2} \cdot \Delta\vec{\mu}_2 \Delta\vec{m}_1 \sin(2\nu) + \frac{1}{2} \sin(2\nu) \cdot \pi \tilde{\nu}_0 \vec{T}_{12} (\Delta\vec{\mu}_1 \times \Delta\vec{\mu}_2)$$

$$R^+ = \Delta\vec{\mu}_1 \Delta\vec{m}_1 \cos^2(\nu) + \frac{1}{2} \cdot \Delta\vec{\mu}_2 \Delta\vec{m}_1 \sin(2\nu) - \frac{1}{2} \sin(2\nu) \cdot \pi \tilde{\nu}_0 \vec{T}_{12} (\Delta\vec{\mu}_1 \times \Delta\vec{\mu}_2) \quad (4)$$

where  $\Delta\vec{m}_1$  is the intrinsic magnetic transition dipole moment associated with the C-terminal amide I. For  $\Delta\vec{m}_1 \neq 0$  one obtains an asymmetric VCD couplet as accounted for by the respective first term in the above equations. The second terms describe cross-coupling between the peptide groups and account for a modification of the symmetric couplet. The band shape of the amide I couplet is modeled by Gaussian profiles as described by Eker et al.<sup>21</sup>

For all peptides investigated, the respective amide I band at lower wavenumbers could be assigned to the out-of-phase combination of the two coupled amide I modes and is therefore labeled as AI<sub>-</sub>. The corresponding band at higher wavenumbers represents the in-phase combination and is designated as AI<sub>+</sub>.

**Spectroscopy.** The experimental setups and instruments used for our Raman, FTIR, and VCD experiments are given in earlier publications.<sup>14</sup> All spectra were analyzed using the program MULTIFIT.<sup>22</sup> For tripeptides in D<sub>2</sub>O, the spectra were normalized to the internal standard, i.e., the ClO<sub>4</sub><sup>-</sup> band at 934 cm<sup>-1</sup>. To eliminate solvent contributions we measured the solvent reference spectra for IR, VCD, and Raman spectra for both polarizations, which were then subtracted from the corresponding peptide spectra. The intensities of the normalized polarized Raman bands were derived from their band areas. These and the corresponding IR spectra were self-consistently analyzed in that they were fitted with a set of identical frequencies, halfwidths, and band profiles. The isotropic and anisotropic Raman intensities and the depolarization ratios  $\rho$  were calculated as

$$I_{\text{iso}} = I_x - \frac{4}{3} I_y$$

$$I_{\text{aniso}} = I_y$$

$$\rho = \frac{I_x}{I_y} \quad (5)$$

It should be mentioned that in principle  $I_{\text{aniso}}$  should be written as  $2.33 \cdot I_y$ . As in earlier papers,<sup>14,16</sup> we prefer to identify it with  $I_y$  in the depicted figures so that the polarization properties of different lines can be better inferred.

## Results and Discussion

**Comparison of Alanine-Based Tripeptides.** Figure 3 compares the IR and Raman spectra of cationic KAA and SAA with those of AAA and AA<sup>DA</sup> investigated in earlier studies.<sup>16,21</sup> Apparently, the differences between the respective spectra are quantitative rather than qualitative, in that all spectra exhibit the same general features. In the IR spectra the low-frequency amide I band (AI<sub>-</sub>) is dominant, while the high-frequency AI<sub>+</sub> band is most intense in the isotropic Raman spectra. In all anisotropic Raman spectra both bands exhibit comparable intensities. These intensity distributions are diagnostic of a



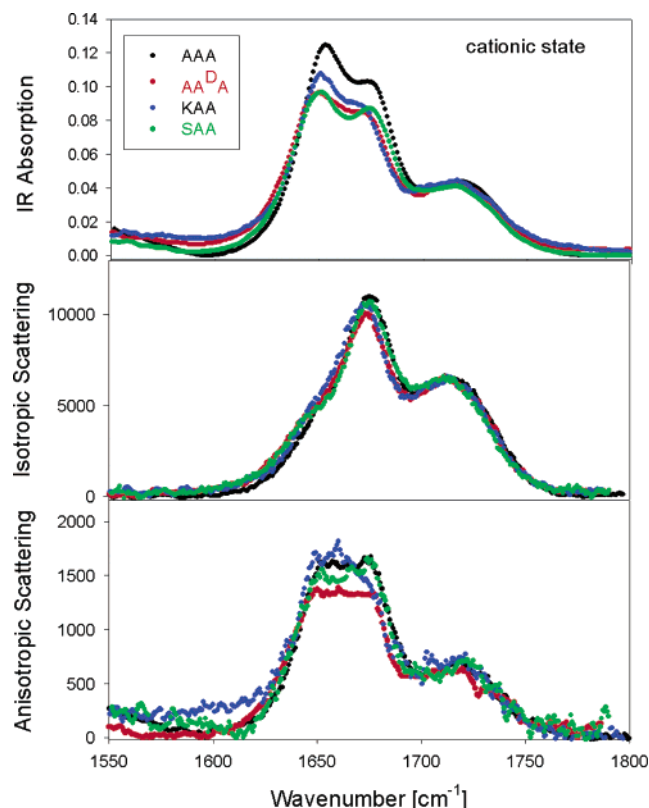


**Figure 3.** FTIR, isotropic, and anisotropic Raman spectra of cationic AAA (black) and AA<sup>D</sup>A (red), KAA (blue), SAA (green) in D<sub>2</sub>O between 1550 and 1800 cm<sup>-1</sup>. The AAA spectra were taken from Schweitzer-Stenner,<sup>16</sup> the AA<sup>D</sup>A spectra from Eker et al.<sup>21</sup> The corresponding polarized Raman spectra of KAA, SAA were measured with 457 nm excitation (laser power: 200 mW, 1 W, 200 mW respectively, sample concentrations: 0.2 M)

structure assignable either to the upper left or the lower right square of the Ramachandran plot.<sup>14,12</sup> The isotropic Raman spectra are particularly similar, indicating that the degree of excitonic mixing between the excited vibrational states is nearly identical for all peptides investigated. Differences between the respective IR and anisotropic Raman spectra are more pronounced. This suggests that the orientations between the peptide groups are somewhat different.

We subjected the spectra of KAA and SAA to a self-consistent spectral decomposition to obtain the intensity ratios  $R_{\text{iso}}$ ,  $R_{\text{aniso}}$ , and  $R_{\text{IR}}$  (Table 2). To give an example, Figure 4 shows the fit and the two amide I bands in the spectra of cationic SAA. Then, we employed the algorithm reported by Schweitzer-Stenner<sup>16</sup> to determine the dihedral angles by which these values can be reproduced. This yields eight possible  $\phi, \psi$  pairs for each tripeptide, but six of them can be fairly well excluded because they are associated with sterically forbidden regions of the Ramachandran plot. One can also demonstrate that they are not consistent with the respective VCD spectra to be discussed below. Hence, we are left with two possible solutions: the respective  $\phi, \psi$  values are both in the upper left square of the Ramachandran space.

It should be notified that our recent paper<sup>16</sup> mentions only four solutions for AAA, two for each of the obtained angles  $\theta_1$  and  $\theta_2$ . We overlooked that one can nearly exchange the numbers of a solution  $(\phi, \psi)$  to obtain a second solution  $(\phi', \psi')$  with  $\phi' \approx -\psi$  and  $\psi' \approx -\phi$  in the same square of the Ramachandran plot. However, as already reported in ref 21, one of these solutions can be disregarded by virtue of the corresponding VCD signal, so that the solution reported in ref

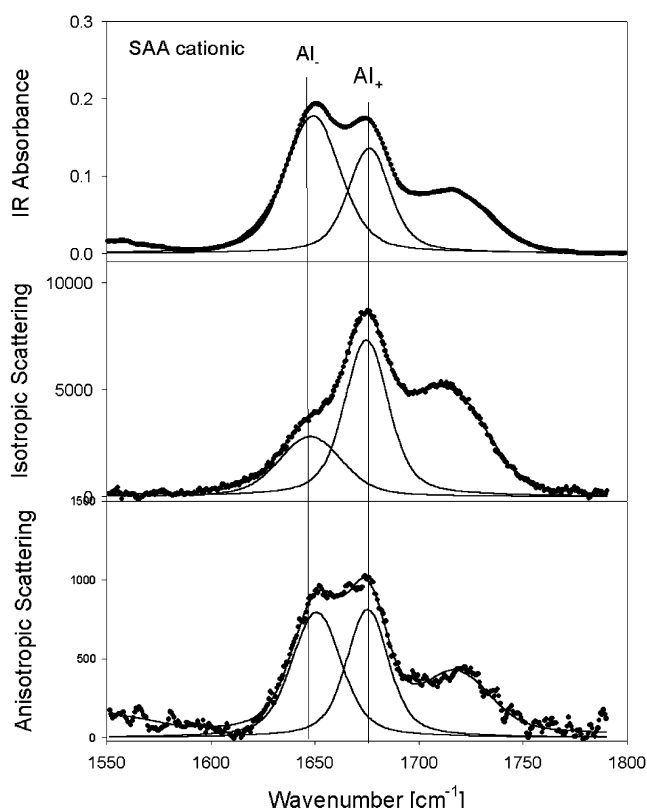


**Figure 4.** FTIR, isotropic and anisotropic Raman spectra of acid (pD = 1) SAA between 1550 and 1800 cm<sup>-1</sup>. The Raman spectra were measured with 457 nm excitation (laser power: 200 mW; sample concentration: 0.2 M). The solid lines and the band profiles result from the spectral fitting described in the text.

16 is correct. Here, we demonstrate this by calculating the VCD signal of amide I for both solutions. The result is depicted in Figure 5a. Amide I shows a couplet with a stronger negative signal at the AI position. The solid line results from a calculation for  $(\phi, \psi)_1 = (-125^\circ, 178^\circ)$ . Two different mechanisms contribute to the couplet. A “coupled oscillator” mechanism described by the respective third terms in eq 4 (cf. Material and Methods) gives rise to a symmetric couplet that is larger than the experimental signal of AI<sub>+</sub> but smaller at the AI position (dashed line in Figure 5a). This signal is slightly modified by the cross-coupling mechanism accounted for by the  $\Delta\vec{m}_1\Delta\vec{\mu}_2$  terms in eq 4. The asymmetry of the signal results from the intrinsic rotational strength of the C-terminal amide I which is associated with a magnetic moment  $\Delta\vec{m}_1 = 2.3 \times 10^{-43}$  esu cm. It adds significant negative rotational strength to the AI state (dotted line in Figure 5a). This interferes constructively with the negative signal from the coupled oscillator coupling and destructively with the corresponding positive signal. Thus, a highly asymmetric VCD signal is produced.

The situation is different for the second solution, i.e.,  $(\phi, \psi)_2 = (-175^\circ, 115^\circ)$ . Figure 5b displays the VCD signal for this geometry. The symmetric couplet of the coupled oscillator is much weaker (dashed line). To reproduce the experimental couplet, one has to rule out any contribution of  $\Delta\vec{m}_1$  to the AI<sub>+</sub> state. This renders the assumed geometry impossible. Any fit which reproduces the negative AI signal gives also rise to an overall negative signal at AI<sub>+</sub>, similar to what has recently been experimentally obtained for triline. Thus, the VCD spectrum of amide I provides the means to select  $(\phi, \psi)_1$  as the valid solution, in agreement with Schweitzer-Stenner.<sup>16</sup>

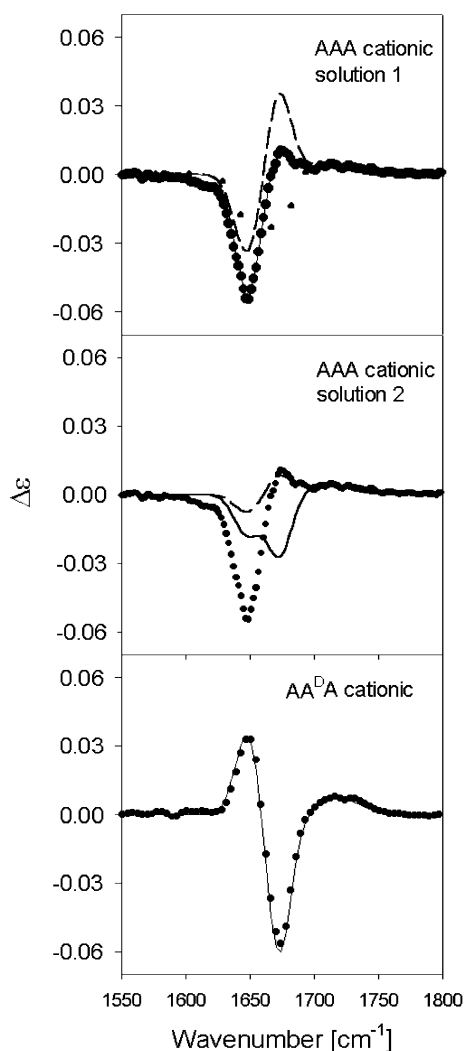


**Figure 5.** Vibrational circular dichroism spectra of cationic AAA and AA<sup>D</sup>A in D<sub>2</sub>O (sample concentrations: 0.3 M, 0.2 M, respectively). The solid and dashed lines result from calculations described in the text.

The amide I VCD signal can also be utilized to confirm the recently reported structure of AA<sup>D</sup>A. While the IR and Raman spectra of cationic AAA and AA<sup>D</sup>A are very similar (Figure 3), the amide I VCD signals are qualitatively different (Figure 3c) in that the AA<sup>D</sup>A couplet is negative at AI<sub>+</sub> and positive at AI<sub>-</sub>. This indicates that the structure of AA<sup>D</sup>A is assignable to the lower left square of the Ramachandran space, as expected. Again, we obtained two solutions, namely  $(\phi, \psi)_1 = (115^\circ, -175^\circ)$  and  $(\phi, \psi)_2 = (170^\circ, -120^\circ)$ , but only the latter reproduces the VCD couplet (solid line in Figure 5c). It should be noted that the stronger negative signal at AI<sub>+</sub> is still solely caused by excitonic coupling and not by any intrinsic rotational strength of the unperturbed amide mode of the N-terminal peptide.

As already indicated by the similarity of the spectra in Figure 3 the differences between the dihedral angles of cationic AAA, KAA, and SAA are small (Table 1). For KAA, this is confirmed by the fact that the amide I VCD couplet of KAA is nearly indistinguishable from that of AAA (data not shown). The structural differences between the three peptides are nearly exclusively due to changes of  $\psi$ . Our results provide strong evidence that the steric properties of the N-terminal amino acid residue have only a limited impact on the central dihedral angles. Instead, it is likely that local interactions between the central residue with the adjacent peptide groups and with the solvent

determine its dihedral angles. We currently perform a series of measurements on AXA peptides to verify this hypothesis.

Thus far we have assumed that all the investigated peptides adopt a single stable structure in solution. This is somewhat at odds with the conventional wisdom that short peptide fragments are very flexible molecules that are able to sample large parts of the Ramachandran space,<sup>23,24</sup> but our results are generally in line with *ab initio* and DFT calculations on blocked alanine dipeptides which strongly suggest that only one or two conformers are stabilized in water.<sup>25,26</sup> Han et al.<sup>25</sup> performed DFT calculations on an alanine dipeptide in water and found nearly identical energies for a PII and a right-handed  $\alpha$ -helical structure. Recently, Mu and Stock<sup>27</sup> reported the first molecular dynamics study on cationic AAA in water and identified three significantly populated conformers exhibiting PII,  $\beta$ -sheet, and  $\alpha_R$ -like structures. In view of these studies the question arises whether the above obtained dihedral angles represent an average structure rather than a stable conformer. In principle, coexisting conformers should give rise to a noncoincidence between isotropic, anisotropic, and IR frequencies due to their different frequency splittings and intensity distributions, as demonstrated for triglycine.<sup>14</sup> A small noncoincidence has indeed been obtained for zwitterionic AAA,<sup>16</sup> but not for the other protonation states of this peptide and the remaining tripeptides investigated. From this observation we can rule out a significant contribution from an  $\alpha$ -helical conformer, since its amide I bands should show a much larger splitting and intensity distribution opposite to those observed.<sup>12</sup> However, in the case of coexisting extended conformers the noncoincidence might be small due to small differences between their coupling energies (cf. the contour plots for  $\Delta$  in the upper left square in Figure 2). Indeed, we have recently shown that the intensity ratios obtained for cationic AAA can be reproduced by a 50:50 mixing between an *assumed* PII ( $(\phi_{\text{PII}}, \psi_{\text{PII}}) = (-60^\circ, 150^\circ)$ ) and an *obtained*, more extended  $\beta$ -sheet-like structure ( $(\phi_\beta, \psi_\beta) = (-160^\circ, 150^\circ)$ ).<sup>21</sup> The latter is somewhat more extended than the  $\beta$  conformation obtained by Mu and Stock ( $(\phi_\beta, \psi_\beta) = (-122^\circ, 130^\circ)$ ),<sup>27</sup> but this is not problematic since the exact structure of this conformer depends on the chosen force field.<sup>28</sup> Our result perfectly reproduces the <sup>3</sup>J-constant for the coupling between the central C $\alpha$ H and the amide proton of the N-terminal peptide.<sup>28</sup> Interestingly, the corresponding experimental data indicate that conformational heterogeneity is nearly absent for other homopeptides such as VVV, SSS, and KKK.<sup>21</sup>

If cationic AAA is heterogeneous one expects that this is also the case for the other cationic alanine based tripeptides investigated in the present study. Indeed, we were able to reproduce also their respective intensity ratios by the above two-state model if one allows slight variations of the dihedral angles (Table 2). Thus, we obtain a 50:50 mixture for AA<sup>D</sup>A and KAA, while the analysis of SAA yields a larger contribution from the extended  $\beta$ -sheet-like structure. In view of the high sheet propensity of serine this seems to be a reasonable result.

We also checked the validity of the two-state model by calculating the amide I VCD signal. A good reproduction of the experimental couplet was always obtained. This results from the fact that the extended structure provides a larger and the PII structure a smaller VCD signal than that measured in the experiment.

One might argue that the obtained intensity ratios reflect a distribution of extended conformers with slightly different amide I frequencies, in line with the conventional view of the conformation dynamics of small peptides. This, however, would give rise to significant inhomogeneous broadening of the amide

I bands. As a consequence, the amide I of corresponding dipeptides should exhibit considerably smaller bandwidths. This, however, is not the case. In fact, the Gaussian bandwidth of amide I in the vibrational spectrum of dialanine in D<sub>2</sub>O is very similar to the corresponding values obtained for trialanine.<sup>14,16</sup>

Very recently, Shi et al.<sup>29</sup> reported a combined electronic CD and NMR study on an acetylated polypeptide with a sequence of seven alanine residues. They showed that this peptide adopts a PII-like structure at room temperature with  $(\phi_{\text{PII}}, \psi_{\text{PII}}) = (-70^\circ, 145^\circ)$ . At higher temperatures this conformer was shown to coexist with a  $\beta$ -sheet-like conformer exhibiting  $(\phi_{\beta}, \psi_{\beta}) = (-135^\circ, 150^\circ)$ . This result is in excellent agreement with our two-conformer model. Moreover, it shows that the conformation of this polypeptide is determined by the structure propensity of its amino acid residues so that a tripeptide adopts structures that are already very comparable to that of longer peptides with the same amino acid composition. The results of Shi et al.<sup>29</sup> and ours strongly suggest that the so-called random coil conformation is not random but ordered with its structure depending on the amino acid composition. In their paper Shi et al.<sup>29</sup> exhibit a frequency plot, which shows the  $\phi, \psi$  distribution of core backbone conformations of nonglycine residues in protein structures. These representations show two maxima in the upper square of the Ramachandran plot which pretty well coincide with the PII and  $\beta$ -structure obtained in the present study.

Various recent spectroscopic experiments have underscored the biological relevance of PII structures, which had been proposed earlier by Tiffany and Krimm.<sup>13</sup> Dukor and Keiderling<sup>30</sup> used VCD spectra of various polypeptides to identify a significant portion of PII structure in what is normally called a random coil state. A CD study of a seven-residue lysine peptide revealed a PII conformation.<sup>31</sup> This parallels findings for another alanine-based water-soluble polypeptide.<sup>32</sup> A very exciting study by Blanch et al.<sup>33</sup> utilized Raman optical activity spectroscopy to show that the amyloidogenic prefibrillar intermediate of human lysozyme exhibits a PII rather than a  $\beta$ -sheet structure. PII also seems to occur in the unfolded state of a series of other proteins associated with neurodegenerative disease.<sup>34</sup> Siligardi and Drake<sup>35</sup> discovered that many peptides reacting with proteins such as B-cell receptors and MHC complexes adopt PII-like structures. Stapley and Creamer<sup>36</sup> performed a survey of a variety of proteins and discovered that short PII motifs can be found in a majority of proteins. They are normally water accessible, in line with the notion that this structure is heavily stabilized by hydrogen bonding with water molecules.<sup>26,37</sup> One would therefore expect that, e.g., AAA switches entirely to an extended  $\beta$ -like conformation in a nonaqueous environment. This is investigated in the following paragraphs.

**AcAA in Water and DMSO-*d*<sub>6</sub>** Figure 6 compares the FTIR and Raman spectra of ionic AcAA (both in D<sub>2</sub>O) and AcAA in DMSO-*d*<sub>6</sub>. The similarity between the spectra of anionic AAA and ionic AcAA<sup>21</sup> suggests that the latter is a good model for the former due to the absence of an N-terminal charge in both molecules. The N-terminal charge is known to have a strong impact on the amide I frequency of the N-terminal peptide.<sup>38,39</sup> Hence, anionic AAA and ionic AcAA are more appropriate models for alanine-based sequences in larger peptides and proteins than AAA species with protonated N-terminals. Unfortunately, however, the respective vibrational spectra of anionic AAA and AcAA are more difficult to analyze, since a reduced splitting cause the two bands to coalesce into a single band with slightly different frequencies in the isotropic and anisotropic Raman spectra. In principle, multiple combinations

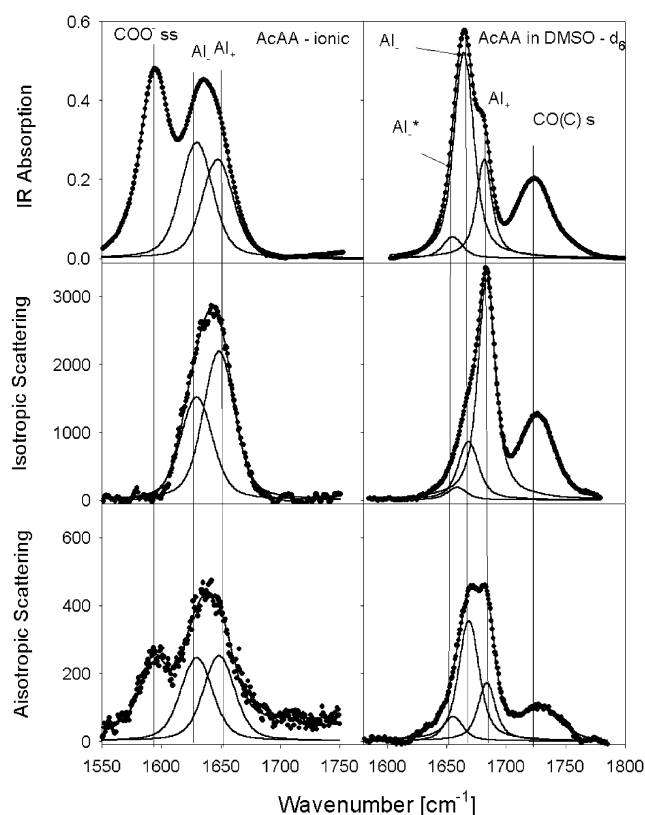


**Figure 6.** FTIR, isotropic, and anisotropic Raman spectra of AcAA in D<sub>2</sub>O (pD = 6.0) (left panel) and DMSO-*d*<sub>6</sub> (right panel) between 1550 and 1750 cm<sup>-1</sup>. The Raman spectra were measured with 457 nm excitation (laser power: 1 W; sample concentration: 0.2 M). The solid lines and the band profiles result from the spectral fitting described in the text.

**TABLE 3: Spectral and Structural Parameters of Anionic AAA<sup>1</sup>, AcAA in D<sub>2</sub>O and DMSO-*d*<sub>6</sub>**

	AAA anion <sup>1</sup>	AcAA D <sub>2</sub> O	AcAA DMSO- <i>d</i> <sub>6</sub>
$\bar{\nu}_-$ [cm <sup>-1</sup> ]	1638	1630	1668
$\bar{\nu}_+$ [cm <sup>-1</sup> ]	1649	1649	1683
$\Gamma_{G-}$ [cm <sup>-1</sup> ] <sup>b</sup>	29.6	25.5	13.0
$\Gamma_{G+}$ [cm <sup>-1</sup> ] <sup>b</sup>	30.5	24.8	7.0
$R_{\text{iso}}$	0.41	0.7	0.33
$R_{\text{aniso}}$	1.1	1.09	1.13
$R_{\text{IR}}$	1.69	1.2	2.47
$\rho_-$	0.28	0.19	0.27
$\rho_+$	0.14	0.14	0.09
$\Delta$ [cm <sup>-1</sup> ] <sup>c</sup>	3.1	1.7	3.7
$\bar{\theta}$	128°	121°	150°
$\theta$	131°	122°	129°
$\phi$	-127	-125	-140
	+8/-4°	+8/-4°	+5/-3°
$\psi$	165	173	125
	+5/-10°	+5/-10°	+5/-3°

<sup>a</sup> Taken from Eker et al.<sup>21</sup> <sup>b</sup> Gaussian halfwidths. <sup>c</sup> Corrected values calculated by using eq 2.

of two bands yield satisfactory and consistent fits to all vibrational spectra. Fortunately, however, only few of them representing pretty small intervals of intensity ratios can be used to obtain dihedral angles by our algorithm. For the majority of the solutions it is impossible to obtain the same  $\phi, \psi$  solution for  $R_{\text{aniso}}$  and  $R_{\text{IR}}$ . Hence, we were able to obtain the dihedral angles of anionic AAA ( $(\phi, \psi) = (-127^\circ, 165^\circ)$ ) and ionic AcAA ( $(\phi, \psi) = (-125^\circ, 173^\circ)$ ) (Table 3),<sup>21</sup> and as expected, they are very similar. They reflect extended, slightly left-handed  $\beta$ -helices such as the single-state structures as obtained for the other protonation states of AAA. Of course, the intensity ratios of

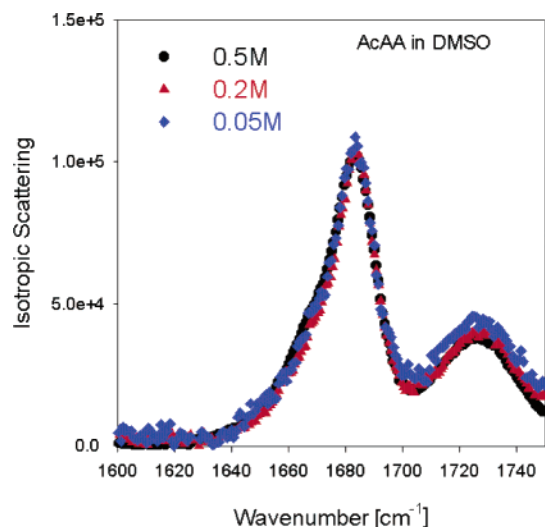


**Figure 7.** Isotropic Raman spectra of AcAA at sample concentration 0.5 M (black), 0.2 M (red), 0.05 M (blue) in D<sub>2</sub>O between 1600 and 1740  $\text{cm}^{-1}$ . The corresponding polarized Raman spectra of AcAA were measured with 457 nm excitation (laser power: 1 W).

both peptides can again be reproduced by the above two-conformer model. However, the two-conformer solution obtained for cationic and zwitterionic AAA was found to be unsuitable to reproduce the VCD spectrum of anionic AAA, which shows a comparatively strong and nearly perfectly symmetric couplet, indicative of a negligible small magnetic moment of the C-terminal peptide. A detailed analysis revealed that any two-conformer model capable of reproducing the observed VCD signal comprises less different structures as those obtained for cationic AAA, i.e., a dominant, somewhat more extended PII with ( $\phi \sim -90^\circ$ ,  $\psi = 150^\circ$ ) and a slightly different  $\beta$ -sheet with  $\phi$ -values between  $140^\circ$  and  $150^\circ$ .

A recent NMR-study by Poon et al.<sup>37</sup> on blocked alanine dipeptides in liquid crystals is noteworthy in this context. This peptide should be considered as a good model for anionic AAA and AcAA. The authors report a single conformer with ( $\phi, \psi$ ) =  $(-85 \pm 5^\circ, 160 \pm 20^\circ)$ . That is very close to the above PII structure of anionic AAA and AcAA and, thus, also not too different from the structure which we obtained from a single-state analysis.

We now consider the spectra of AcAA in DMSO- $d_6$  in the right column in Figure 6. As shown therein, the spectral analysis reveals two discernible amide I bands and another weak band on the low wavenumber side of  $\text{Al}_-$ . To check the aggregation for peptide, we have measured the Raman and IR spectra for different peptide concentrations, i.e., 0.05, 0.2, and 0.5 M. Figure 7 compares the isotropic Raman spectra of the 0.5 M sample with the scaled spectra of the other two samples. The amide I profiles are nearly identical, while the respective CO bands at  $1730 \text{ cm}^{-1}$  show different intensities and slightly different frequencies. This could arise from hydrogen bonding between the C-terminal carbonyl and one of the NH groups of another peptide. Such an interpeptide interaction would give rise to a peptide dimer in which one peptide is approximately perpendicularly oriented to the other one. This configuration would minimize the transition dipole coupling. This is in agreement with the concentration independence of the amide I profile which, even at high concentration, solely reflects the structure of the peptide. We used the 0.5 M spectrum for our analysis to exploit its excellent signal-to-noise ratio. The spectral and structural parameters obtained from the analysis of these spectra are listed in Table 3. To crosscheck the result of our analysis,

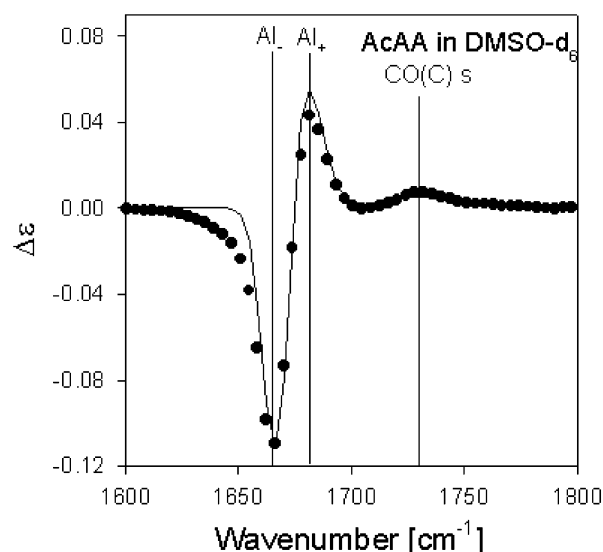


**Figure 8.** Vibrational circular dichroism spectra of AcAA in DMSO- $d_6$  (sample concentration: 0.2 M). The solid and dashed lines result from calculations described in the text.

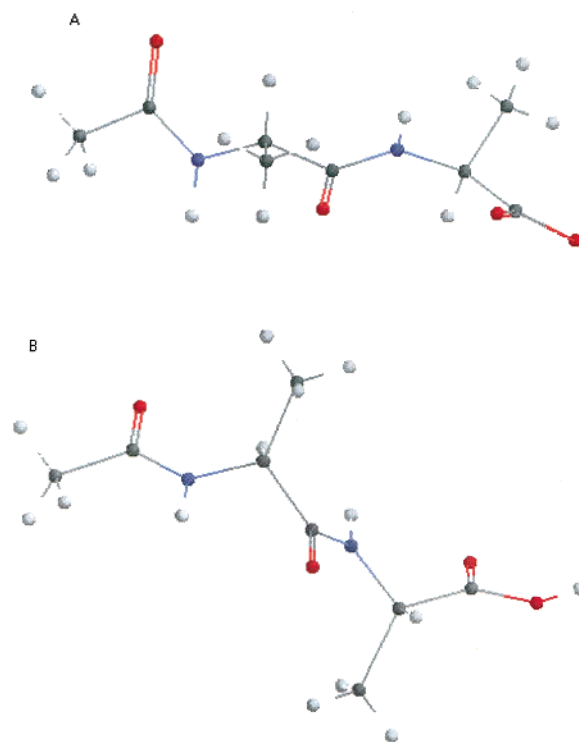


**Figure 9.** Structure of AcAA in D<sub>2</sub>O (anionic state) (A) and in DMSO (neutral state) (B) as obtained from the analysis of the amide I band profiles in IR absorption and Raman scattering.

we also measured and calculated the amide I VCD signal (Figure 8) and observed a good agreement with the experimental data. The deviation at the low wavenumber side of  $\text{Al}_-$  results from our use of pure Gaussian profiles, while the real band profiles are Voigtian.

Our analysis yielded two remarkable results. First, we obtained a nearly perfect  $\beta$ -sheet structure ( $\phi = -140^\circ$ ,  $\psi = 125^\circ$ ), which differs from left-handed helical structure obtained for AcAA in water (PII or  $\beta$ -helix). It is shown in Figure 9. This suggests that the structural propensity of alanine is solvent dependent in that the sheet propensity is apparently supported by a more hydrophobic environment, while the PII structure is supported in water. Our result corroborates the notion that a



PII structure requires an aqueous environment.<sup>26,37</sup> This would make PII an ideal initiation state for a coil  $\rightarrow$  helix transition, which causes a release of the peptide bound water and thus a substantial gain in entropy.<sup>40</sup> Hence, the high helical propensity of alanine would coincide with high propensity for a PII conformation in the so-called "coil state". Of course, further experiments are necessary to confirm this proposal. Second, our spectral analysis revealed that the Gaussian bandwidths of AcAA in DMSO-*d*<sub>6</sub> are significantly smaller than those observed for an aqueous solution, while the Lorentzian part remains nearly unaffected. As a consequence the band profiles of AcAA in DMSO-*d*<sub>6</sub> become Voigtian. This is an important result for two reasons. First, it confirms the result of a recent study by Gnanakaran and Hochstrasser,<sup>41</sup> which suggested that the amide I broadening for peptides in water results mostly from fluctuations of hydrogen bonding with water. Second, it shows that conformational fluctuations do not cause overwhelmingly large inhomogeneous broadening which suggests that it is confined to a pretty limited area around the obtained dihedral angles in the Ramachandran space.

## Conclusion

Taken together, the current study demonstrates the use of vibrational spectroscopy to determine the structure of tripeptides in solution. We could show that alanine based tripeptides adopt stable extended structures assignable to the upper left square of the Ramachandran plot. Our results do not support the notion that small peptides exhibit infinite conformational flexibility. On the contrary, they provide evidence that, e.g., tripeptides are very suitable model systems to study the structural propensity of amino acid residues in different environments. That fits nicely into the picture emerging from investigations on longer alanine based peptides.<sup>29,32</sup> Of particular biological relevance is our finding that the PII conformer obtained for AAA, AcAA, KAA, and SAA (in the one-state as well as in the two-state model, since the  $\beta$ -helix is in fact an extended PII structure) does require water as a solvent and therefore disappears in a nonaqueous environment.

**Acknowledgment.** Financial support for R.S.S. was provided from the NIH-COBRE II grant for the *Center for Research in Protein Structure, Function and Dynamics*, from the NIH SCORE grant (S06 GM008102-3052), and from the Fondos Institucionales para la Investigación of the University of Puerto Rico (20-02-2-78-514). We thank Dr. Brad Weiner for allowing us to build a temporary set up for Raman experiments in his laboratory. R.S.S. thanks Timothy A. Keiderling for very useful discussions concerning the excitonic coupling mechanism for amide I and Peter Hamm and Gerhard Stock for a very intensive e-mail discussion concerning the comparison of spectroscopic and computational studies on cationic trialanine. Both colleagues have provided us reprints and important results (<sup>3</sup>J-coupling) prior to publication. In addition, Peter Hamm has advised us on how to convert force constants reported by Torii and Tasumi.<sup>12</sup> Dr. Torii was so kind to send us the force constants used to calculate the contour plot for the coupling energy in

Figure 2a. The Syracuse authors acknowledge support from the National Institutes of Health grant (GM62848) for financial support.

## References and Notes

- (1) Krimm, S.; Bandekar, J. *Adv. Protein Chem.* **1986**, *38*, 181.
- (2) Chi, Z.; Asher, S. A. *Biochemistry* **1998**, *37*, 2865.
- (3) Griebenow, K.; Santos, S. M.; Carrasquillo, K. G. 1999. *Internet J. Vib. Spectrosc.* 1999; [www.ijvs.com] 3: 1–20.
- (4) Hu, X.; Dick, L. A.; Spiro, T. G. *Biochemistry* **1998**, *37*, 9445–9448.
- (5) Chi, Z.; Asher, S. A. *Biochemistry* **1998**, *37*, 2865.
- (6) Keiderling, T. A. In *Circular Dichroism and the Conformational Analysis of Biomolecules*; Fasman, G. D., Ed.; Plenum Press: New York, 1996.
- (7) Barron, L. D.; Hecht, L.; Blanch, E. W.; Bell, A. F. *Prog. Biophys. Mol. Biol.* **2000**, *73*.
- (8) Barron, L. D.; Blanch, E. W.; McColl, I. H.; Syme, C. D.; Hecht, L.; Nielsen, K. *Spectroscopy*, in press.
- (9) Williams, S.; Causgrove, T. P.; Gilmanshore, R.; Fang, K. S.; Callender, R. H.; Woodruff, W. W.; Dyer, R. B. *Biochemistry* **1996**, *35*, 691.
- (10) Lednev, I. K.; Karnoup, A. S.; Sparrow, M. C.; Asher, S. A. *J. Am. Chem. Soc.* **1999**, *121*, 8074.
- (11) Woutersen, S.; Hamm, P. *J. Phys. Chem. B* **2000**, *104*, 11316.
- (12) Torii, H.; Tasumi, M. *J. Raman Spectrosc.* **1998**, *29*, 81.
- (13) Tiffany, M. L.; Krimm, S. *Biopolymers* **1968**, *6*, 1379.
- (14) Schweitzer-Stenner, R.; Eker, F.; Huang, Q.; Griebenow, K. *J. Am. Chem. Soc.* **2001**, *123*, 9628.
- (15) Woutersen, S.; Hamm, P. *J. Chem. Phys.* **2001**, *114*, 2727.
- (16) Schweitzer-Stenner, R. *Biophys. J.* **2002**, *83*, 523.
- (17) Glasoe, P. K.; Long, F. A. *J. Phys. Chem.* **1960**, *64*, 188.
- (18) Sieler, G.; Schweitzer-Stenner, R. *J. Am. Chem. Soc.* **1997**, *119*, 1720.
- (19) The corresponding eqs 5 and 6 in refs 16 and 14 are incorrect. They yield an underestimation of the coupling energy.
- (20) Holzwarth, G.; Chabay, I. *J. Chem. Phys.* **1972**, *57*, 1632.
- (21) Eker, F.; Cao, X.; Nafie, L.; Schweitzer-Stenner, R. *J. Am. Chem. Soc.* **2002**, *124*, 14330.
- (22) Jentzen, W.; Unger, E.; Karvounis, G.; Shelnutt, J. A.; Dreybrodt, W.; Schweitzer-Stenner, R. *J. Phys. Chem.* **1996**, *100*, 14184.
- (23) Zimmermann, S. S.; Pottle, M. S.; Némethy, G.; Scheraga, H. *Macromolecules* **1977**, *10*, 1.
- (24) Wright, P. E.; Dyson, H. J.; Lerner, R. A. *Biochemistry* **1988**, *27*, 7167.
- (25) Shang, H. S.; Head-Gordon, T. *J. Am. Chem. Soc.* **1994**, *116*, 1528.
- (26) Han, W. G.; Jalkanen, K. J.; Elstner, M.; Suhai, S. *J. Phys. Chem. B* **1998**, *101*, 2587–2602.
- (27) Mu, Y.; Stock, G. *J. Phys. Chem. B* **2002**, *106*, 5294.
- (28) Mu, Y.; Kosov, D. S.; Stock, G., submitted for publication.
- (29) Shi, Z.; Olson, Z. A.; Rose, D. G.; Baldwin, R. L.; Kallenbach, N. R. *Proc. Natl. Acad. Sci. U.S.A.* **2002**, *99*, 9190.
- (30) Dukor, R. K.; Keiderling, T. A. *Biopolymers* **1991**, *31*, 1747.
- (31) Rucker, A. L.; Creamer, T. P. *Protein Sci.* **2002**, *11*, 980.
- (32) Park, S. H.; Shalongo, W.; Stellwagen, E. *Protein Sci.* **1997**, *6*, 1694.
- (33) Blanch, E. W.; Morozova-Roche, L. A.; Crochan, D. A. E.; Doig, A. J.; Hecht, L.; Barron, L. D. *J. Mol. Biol.* **2000**, *301*, 553.
- (34) Syme, C. D.; Blanch, E. W.; Holt, C.; Jakes, R.; Goedert, M.; Hecht, L.; Barron, L. D. *Eur. J. Biochem.* **2002**, *269*, 148.
- (35) Siligardi, G.; Drake, A. F. *Biopolymers* **1995**, *37*, 281.
- (36) Stapley, B. T.; Creamer, T. P. *Protein Sci.* **1999**, *8*, 587.
- (37) Poon, C. D.; Samulsi, E. T.; Weise, C. F.; Weisshaar, J. C. *J. Am. Chem. Soc.* **2000**, *122*, 5642.
- (38) Sieler, G.; Schweitzer-Stenner, R.; Holtz, J. S. W.; Pajcini, V.; Asher, S. A. *J. Phys. Chem. B* **1999**, *103*, 372.
- (39) Schweitzer-Stenner, R. *J. Raman Spectrosc.* **2001**, *32*, 711.
- (40) Auror, R.; Creamer, T. P.; Srinivasa, R.; Rose, G. D. *J. Biol. Chem.* **1997**, *272*, 1413.
- (41) Gnanakaran, S.; Hochstrasser, R. M. *J. Am. Chem. Soc.* **2001**, *123*, 12886.